Current instability in field-effect transistors: influence of magnetic field and collisions

2001 J. Phys.: Condens. Matter 13 10105

(http://iopscience.iop.org/0953-8984/13/44/321)

INSTITUTE OF PHYSICS PUBLISHING JOURNAL OF PHYSICS: CONDENSED MATTER

J. Phys.: Condens. Matter **13** (2001) 10105–10116 PII: S0953-8984(01)24828-0

Current instability in field-effect transistors: influence of magnetic field and collisions

M S Kushwaha[1] **and P Vasilopoulos**

Department of Physics, Concordia University, 1455 de Maisonneuve Boulevard West, Montreal, Quebec, Canada H3G 1M8

Received 15 May 2001, in final form 24 August 2001
Published 19 October 2001
Online at stacks.iop.org/JPhysCM/13/10105

Abstract

A theoretical investigation is made of the plasma-wave instability mechanism in a two-dimensional (2D) electron fluid in a field-effect transistor (FET) in the presence of a perpendicular magnetic field. The influence of electron collisions with impurities and/or phonons is also taken into account. The 2D electron fluid in the FET channel is treated within the framework of hydrodynamics. The treatment is valid for a nondegenerate electron fluid in which the mean free path for interelectronic collisions is much smaller than the device length and the mean free path due to impurities and/or phonons. It is shown that a relatively low direct current should be unstable because of magnetoplasma-wave amplification due to the reflection of the wave from the device boundaries. The role of an applied magnetic field is *additive*: the greater the magnetic field, the larger the wave increment. In that sense an applied magnetic field may be used to compensate (or overcome) the *subtractive* role played by collisions on plasma-wave generation. Such a ballistic FET is promising for the generation of tunable electromagnetic radiation in the terahertz frequency range.

1. Introduction

The past two decades have seen a great deal of research effort in the investigation of semiconducting systems of reduced dimensionality. As the dimensions of semiconductor devices get smaller, the probability that electrons can traverse them without scattering at all, i.e., ballistically, increases. Under such conditions the transport of electrons in the solid resembles that in vacuum, but with the effective mass and group velocity of the electrons in the semiconductor. A classic, purely ballistic transport model in a planar n–i–n structure was first proposed by Shur and Eastman [1]. Experimental observation of ballistic effects primarily involved vertical devices called hot-electron transistors [2]. An earlier review of the subject, both experimental and theoretical, can be found in reference [3].

[1] Permanent address: Institute of Physics, University of Puebla, PO Box J-45, Puebla 72570, Mexico.

0953-8984/01/4410105+12$30.00

Subsequently, Dyakonov and Shur [4] demonstrated that a relatively low direct current in a ballistic field-effect transistor (FET) may become unstable. This instability was interpreted as being a result of the plasma-wave amplification due to the wave's reflection from the device boundaries. It was argued that this provides a practically realizable mechanism for the generation of tunable electromagnetic radiation in the terahertz frequency range. It is noteworthy that the theoretical explanation of the said effect was based on the fact that the mean free path for electron–electron scattering, λ_{ee}, in a FET may be much smaller than the channel length, L, as well as than the mean free path for electron collisions with impurities and/or phonons, λ_{coll}, which determine the electron mobility in the device. Consequently, the electrons in a FET channel behave like a fluid describable on the basis of the hydrodynamics for shallow water. In this analogy the plasma waves in the FET channel play the role of shallow water waves. It should be pointed out that the instability criterion predicted in reference [4] was noticed in the linear approximation.

Later, the same authors [5] investigated a mechanism of current saturation in a FET caused by the choking of electron flow, similar to that of a gas flow in a pipe [6]. It was shown that the choking phenomenon in the samples should lead to a large variation in the current–voltage characteristics. While Dyakonov and Shur [4] limited their analysis to the linear approximation, Gelmont [7] embarked on consideration of the nonlinear evolution of the current instability in a ballistic FET in the case where the electron fluid velocity was closer to the plasma-wave velocity. However, he concentrated on an idealized situation where the viscosity of the electron fluid, associated with electron–electron scattering, and collisions with impurities and/or phonons were absent. These effects are also, respectively, termed the internal friction and external friction. For this case, Gelmont demonstrated that discontinuities in the distribution of the electron concentration and velocity may be formed in the FET channel which are analogous to hydraulic jumps [8].

Similar efforts in studying the nonlinear evolution of the current instability in a ballistic FET were made by Furman and collaborators [9,10]. They considered the case of relatively low electron–fluid velocity and also incorporated the effects of external and internal frictions. It was demonstrated that the occurrence of the instability leads to the establishing of small-amplitude stationary oscillations with amplitude proportional to the square root of the increment.

Conceptual diagnoses of the current instability in a 2D electron fluid in a high-electron-mobility transistor (HEMT) are already becoming known to have paved the way to its wide applications in a new generation of terahertz devices [11]. Examples include sources, detectors, mixers, multipliers, and oscillators. The experimental and theoretical details of how the propagation of plasma waves in a HEMT can be used to realize such plasma-wave electronic devices operating at terahertz frequencies can be found in reference [11]. It is believed that the HEMT-based sources or detectors utilizing plasma waves should operate at much higher frequencies than the conventional transit-time-limited devices. This is simply because the plasma waves propagate much faster than electrons. Shur and collaborators estimate that these terahertz devices should outperform the conventional terahertz devices, which use deep-submicron Schottky diodes.

The purpose of this paper is to investigate the influence of a magnetic field, applied perpendicularly to the 2DEG, and the external friction on the current instability mechanism in a GaAs-based ballistic FET channel (figure 1). While the external friction accounts for nonzero temperature effects in a realistic situation, an external magnetic field introduces an additional length scale, the magnetic length $\ell_c = \sqrt{\hbar/m\omega_c}$, which may (and usually does) give deeper insight into the problem. The rest of the physical conditions associated with the 2DEG in a short FET channel are assumed to be the same as in reference [4] so that the 2DEG is describable within the laws of hydrodynamics. For this to be the case the magnetic field

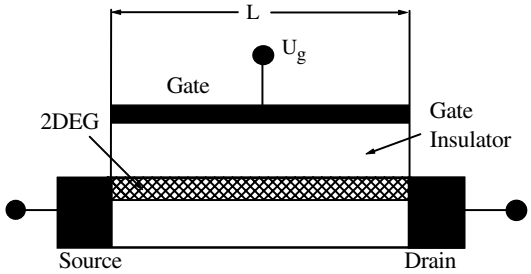

Figure 1. A schematic diagram of a FET. The mean free path for electron–electron scattering λ_{ee}, the gate length L, and the mean free path for electron collisions with impurities and/or phonons λ_{coll} satisfy the inequality $\lambda_{ee} \ll L \ll \lambda_{coll}$.

must be sufficiently *weak*. With explicit illustrative examples, we demonstrate that an applied magnetic field can not only overcome the *subtractive* role played by the external friction, but also modify the direct-current instability in a FET channel over the regime of parameters investigated.

The rest of the paper is organized as follows. In section 2 we present the formalism and derive the final expression employed to study the instability mechanism. In section 3 we present a few illustrative examples. Finally, in section 4 we present a brief discussion of the results and pinpoint some dimensions worth adding to the problem in the future.

2. Formalism

In this paper we will limit ourselves to the case where the internal friction is zero. We first treat the case where the external friction is treated exactly and the magnetic field is zero. Then we generalize the treatment to include the magnetic field exactly and consider the external friction in a reasonably approximate way.

2.1. Zero magnetic field

We start with the hydrodynamic equations for the 2D electrons with a dissipative term νV, which describes the electron collisions with impurities and/or phonons:

$$\frac{\partial V}{\partial t} + V\frac{\partial V}{\partial x} + \nu V = -\frac{e}{m}\frac{\partial U}{\partial x} \tag{1}$$

where $V(x,t)$ is the local hydrodynamic electron velocity. Here $U = U_{gc}(x) - U_T$; U_{gc} is the local gate-to-channel voltage swing, U_T is the threshold voltage, and $\partial U/\partial x$ is the longitudinal electric field in the channel. The phenomenological relaxation time $\tau = \nu^{-1}$ accounts for electron scattering by the impurities and/or phonons. Equation (1) is analogous to the hydrodynamic Navier–Stokes equation, with U corresponding to the shallow water level and V to the local velocity of the water flow. Equation (1), usually termed the Euler equation of motion, has to be solved together with the equation of continuity

$$\frac{\partial U}{\partial t} + \frac{\partial (UV)}{\partial x} = 0. \tag{2}$$

The surface carrier concentration n_s in the FET channel is given by

$$n_s = CU/e \tag{3}$$

where C is the gate capacitance per unit area and e is the electron charge. Equation (3) represents the gradual channel approximation [4], which is valid when the characteristic scale of the potential variation in the channel is much greater than the gate-to-channel separation d. Note that equation (3) was used in writing equation (2).

Now we consider the situation where the source and drain are connected to a current source and the gate and source are connected to a voltage source, U_{GS}. This corresponds to a constant value of the potential at the source ($x = 0$) and to a constant value of the current at the drain ($x = L$). These boundary conditions correspond to zero impedance at the source and an infinite impedance at the drain and are analogous to those for a transmission line, short-circuited at one end and open at the other. However, in contrast to the transmission line, the plasma-wave velocities in our system differ for the opposite directions of propagation. Our purpose here is to show that this velocity difference leads to the instability of the steady electron flow with respect to the plasma-wave generation. To this end we will embark on studying the temporal behaviour of a small fluctuation superimposed on a steady uniform flow.

We linearize equations (1) and (2) by setting

$$V = V_0 + V_1 \exp(-\mathrm{i}\omega t) \qquad U = U_0 + U_1 \exp(-\mathrm{i}\omega t).$$

The result is a set of two coupled equations for the unknowns V_1 and U_1. These unknowns are then allowed a spatial dependence of the form

$$Q = R\mathrm{e}^{\lambda x} \tag{4}$$

where $Q(R) \equiv V_1(\overline{V}_1), U_1(\overline{U}_1)$; this leads to the set of equations

$$(\lambda V_0 - \mathrm{i}\omega + \nu)\overline{V}_1 + \lambda(e/m)\overline{U}_1 = 0 \tag{5}$$

and

$$\lambda U_0 \overline{V}_1 + (\lambda V_0 - \mathrm{i}\omega)\overline{U}_1 = 0. \tag{6}$$

For a nontrivial solution, the determinant of the coefficients must vanish. This leads to

$$(\lambda V_0 - \mathrm{i}\omega)(\lambda V_0 - \mathrm{i}\omega + \nu) - s^2\lambda^2 = 0 \tag{7}$$

where $s = (eU_0/m)^{1/2}$ is the plasma-wave velocity. It is convenient to solve for λ from equation (7) in terms of the effective wavenumber $k = \omega/s$ and the Mach number $r_0 = V_0/s$. We write

$$\lambda_{1,2} = \pm\frac{\mathrm{i}}{2(1-r_0^2)}\left[\sqrt{(k-k')^2 r_0^2 + 4kk'} \mp (k+k')r_0\right] \tag{8}$$

where $k' = k + \mathrm{i}k_\nu$, with $k_\nu = \nu/s$. Applying the boundary conditions expressed in the forms $U(0,t) = U_0$ and $U(L,t)V(L,t) = U_0V_0$ yields

$$\beta_1 \mathrm{e}^{\lambda_1 L} - \beta_2 \mathrm{e}^{\lambda_2 L} = 0 \tag{9}$$

where

$$\beta_i = (\lambda_j r_0 - \mathrm{i}k')\left[\lambda_i(1-r_0^2) + \mathrm{i}k' r_0\right] \tag{10}$$

and $i, j \equiv 1, 2$. Equation (9) is further simplified to give

$$\mathrm{e}^{2(\lambda_{1r} - \lambda_{2r})L} - (a^2 + b^2)/c^2 = 0 \tag{11}$$

where

$$a = \beta_{1r}\beta_{2r} + \beta_{1i}\beta_{2i} \qquad b = \beta_{1r}\beta_{2i} - \beta_{2r}\beta_{1i} \qquad c = \beta_{1r}^2 + \beta_{1i}^2.$$

Here λ_{jr} is the real part of λ_j, $j \equiv 1, 2$. Similarly, β_{jr} (β_{ji}) is the real (imaginary) part of β_j. Equation (11) is the one that is solved at the computational level. This is a transcendental

function which is obtained by substituting $k = k_r + \mathrm{i}k_i$ where k_r and k_i are the real and imaginary parts of k, respectively. Thus equation (11) is an expression where a group of four parameters, r_0, k_v, k_r, and k_i, are inseparably interwoven.

In the absence of external friction, i.e., for $k' = k$, equation (8) simplifies to

$$\lambda_{1,2} = \pm\frac{\mathrm{i}k}{(1 \pm r_0)} \tag{12}$$

and equation (10) reduces to

$$\beta_{1,2} = \pm\frac{k^2}{(1 \mp r_0)}. \tag{13}$$

Then equation (9) assumes the form

$$\mathrm{e}^{(\lambda_1-\lambda_2)L} + \frac{1 - r_0}{1 + r_0} = 0. \tag{14}$$

This equation when further solved yields two independent expressions:

$$k_r = \frac{|1 - r_0^2|}{2L}\pi n \tag{15}$$

where n is an integer including zero, and

$$k_i = \frac{1 - r_0^2}{2L}\ln\left|\frac{1 + r_0}{1 - r_0}\right|. \tag{16}$$

Equations (15) and (16) are exactly the same as equations (4) and (5) in reference [4]. It is a simple matter to understand that $r_0 = \pm 1$ and $r_0 = 0$ imply zero instability in the system.

2.2. Nonzero magnetic field

In this case we start with the hydrodynamic equations for 2D electrons in the presence of an applied magnetic field $\vec{B}$ giving rise to the Lorentz force $e(\vec{V} \times \vec{B})$:

$$\frac{\partial \vec{V}}{\partial t} + \vec{V} \cdot \vec{\nabla}\vec{V} + \nu\vec{V} = \frac{e}{m}\left[-\vec{\nabla}U + \vec{V} \times \vec{B}\right]. \tag{17}$$

Equation (17) has to be solved together with the equation of continuity,

$$\frac{\partial U}{\partial t} + \vec{\nabla} \cdot (U\vec{V}) = 0. \tag{18}$$

Notice that equations (17) and (18) are vectorial, due to the presence of the Lorentz force, in contrast with equations (1) and (2) which are scalar. Just as before, we will limit ourselves to the consideration of the magnetoplasma waves and demonstrate that such waves may grow in time due to reflections from the device boundaries under boundary conditions specific to a FET channel. The description provided by equations (17) and (18) is valid only for *weak* magnetic fields for which Landau quantization is absent.

We fix the orientation of the applied magnetic field such that $\vec{B} \parallel \hat{z}$-direction, and linearize equations (17) and (18) just as before. Then we obtain a set of three equations, from equations (17) and (18), in terms of three unknowns: V_{1x}, V_{1y}, and U_1. These three unknowns are then allowed a spatial dependence of the form

$$I = J\mathrm{e}^{\lambda(x+y)} \tag{19}$$

where $I(J) \equiv V_{1x}(A)$, $V_{1y}(B)$, and $U_1(C)$. We take the same 'damping constant' λ along x and y mostly for mathematical tractability. This is also a reasonable approximation in the linear regime, i.e., as long as the source–drain field $\propto \partial U/\partial x$ is small.

The resulting equations for the coefficients A, B, and C, in matrix form, are

$$\begin{bmatrix} (\alpha_1 + 2\alpha_2\lambda) & -\alpha_3 & \alpha_4\lambda \\ \alpha_3 & (\alpha_1 + 2\alpha_2\lambda) & \alpha_4\lambda \\ \alpha_5\lambda & \alpha_5\lambda & (1 + 2\alpha_2\lambda) \end{bmatrix} \begin{bmatrix} A \\ B \\ C \end{bmatrix} = \begin{bmatrix} 0 \\ 0 \\ 0 \end{bmatrix} \tag{20}$$

where

$$\alpha_1 = 1 + \mathrm{i}\gamma \qquad \alpha_2 = \mathrm{i}V_0/\sqrt{2}\,\omega \qquad \alpha_3 = \mathrm{i}\omega_c/\omega \qquad \alpha_4 = \mathrm{i}e/m\omega \qquad \alpha_5 = \mathrm{i}U_0/\omega.$$

Here, $\omega_c = eB/m$ is the electron cyclotron frequency and $\gamma = \nu/\omega$. For a nontrivial solution of this set of equations the determinant of the coefficients must vanish. The result is

$$(1 + 2\alpha_2\gamma)\left[(\alpha_1 + 2\alpha_2\lambda)^2 + \alpha_3^2 - 2\alpha_4\alpha_5\lambda^2\left(1 + \frac{\mathrm{i}\gamma}{1 + 2\alpha_2\lambda}\right)\right] = 0. \tag{21}$$

We neglect the term $\mathrm{i}\gamma/(1 + 2\alpha_2\lambda)$ and write

$$(1 + 2\alpha_2\gamma)\left[(\alpha_1 + 2\alpha_2\lambda)^2 + \alpha_3^2 - 2\alpha_4\alpha_5\lambda^2\right] \simeq 0. \tag{22}$$

This approximation not only allows us to get rid of the complexity of solving a cubic equation, hence leaving us mostly with a numerical solution of the problem, but also provides us with reasonable grounds for having a physical feeling for the external friction in the problem. Obviously it is reasonable approximation when γ is very small. Either the first $(\cdots)$ or the second $[\cdots]$ factor in equation (22) is zero. Equating the first factor to zero gives

$$\lambda = \frac{\mathrm{i}}{\sqrt{2}}\frac{\omega}{V_0}. \tag{23}$$

This root, which is independent of the collisional frequency ν, the plasma-wave velocity s, and the cyclotron frequency ω_c, is of no interest. Equating the square bracket in equation (22) to zero yields

$$\lambda_{1,2} = \frac{1}{2p}\left[-q \pm \sqrt{q^2 - 4pr}\right] \tag{24}$$

where p, q, and r are, in general, complex quantities defined by

$$p = 2(2\alpha_2^2 - \alpha_4\alpha_5) \qquad q = 4\alpha_1\alpha_2 \qquad r = \alpha_3^2 + \alpha_1^2.$$

It is not difficult to understand the special limits of (i) $\gamma = 0$ and (ii) $B = 0$ and $\gamma = 0$. In the first case, which implies $\alpha_1 = 1$, one is left with

$$\lambda_{1,2} = \pm\frac{\mathrm{i}k}{\sqrt{2}(1 - r_0)}\left[\sqrt{1 - \frac{k_c^2}{k^2}(1 - r_0^2)} \mp r_0\right] \tag{25}$$

where $k_c = \omega_c/s$. Imposing further the limit of zero magnetic field ($\Rightarrow k_c = 0$) and thereby expecting to obtain equation (12) requires replacing $\sqrt{2}\,\lambda$ by λ. In the presence of the Lorentz force, which makes the basic equations vectorial, such a situation prevails simply because we are considering the dynamical variables (i.e., velocity, propagation vector, etc) along both $\hat{x}$- and $\hat{y}$-directions, as well as their dependences. The situation simplifies considerably in the zero-field case because there the $\hat{y}$-direction plays no role at all. Remember, both solutions in equation (25) have to be matched while applying the proper boundary conditions expressed as $U_1(x = 0) = 0$ and $\Delta j(x = L) = 0$, which are equivalent to $U(0, t) = U_0$ and $U(L, t)V(L, t) = U_0V_0$, respectively. Physically speaking, they express the fact that the potential is constant at the source ($x = 0$) and the current is constant at the drain ($x = L$). Since we consider an infinite system along y, or at least one with an extent much larger than the magnetic or any other relevant length, the system is uniform along y and these conditions, resulting from the asymmetry due to the source–drain field, are sufficient. However, if we were

to evaluate the Hall field E_y, in the linear regime, we would impose the condition $j(y) = 0$. This would connect the Hall field along y with $j(x)$ since $E_y \propto j(x)$ and thus the wave reflection from the y-boundaries with that from the x-boundaries. This will be the subject of a separate study.

Applying these boundary conditions yields

$$\delta_1 e^{\lambda_1 L} - \delta_2 e^{\lambda_2 L} = 0 \tag{26}$$

where

$$\delta_i = \frac{2\alpha_2\lambda_i(\alpha_1 + \alpha_2\lambda_i) - (1 + 2\alpha_2\lambda_i)(\alpha_1 + \alpha_2\lambda_i + \alpha_3)}{\lambda_i(\alpha_1 + 2\alpha_2\lambda_i)} \tag{27}$$

and $i \equiv 1, 2$. With further manipulation equation (26) is rewritten as

$$e^{2(\lambda_{1r} - \lambda_{2r})L} - (A^2 + B^2)/C^2 = 0 \tag{28}$$

where

$$A = \delta_{1r}\delta_{2r} + \delta_{1i}\delta_{2i} \qquad B = \delta_{1r}\delta_{2i} - \delta_{2r}\delta_{1i} \qquad C = \delta_{1r}^2 + \delta_{1i}^2.$$

Here λ_{jr} is the real part of λ_j, $j \equiv 1, 2$. Similarly, δ_{jr} (δ_{ji}) is the real (imaginary) part of δ_j. Equation (28) is the final expression employed to investigate direct-current instability in the ballistic FET channel in the presence of a perpendicular magnetic field and the external friction. This is a transcendental function where a group of five parameters (i.e., r_0, k_v, k_c, k_r, and k_i) are inseparably interwoven, unlike in the zero-B and zero-ν case where the explicit expressions for k_r and k_i are decoupled from each other; cf. equations (15) and (16).

3. Illustrative examples

Figure 2 shows the wave increment k_i as a function of the Mach number $r_0 = V_0/s$. As indicated in the figure, the solid, dashed, dash–dotted, dash–dot–dotted, and dotted curves

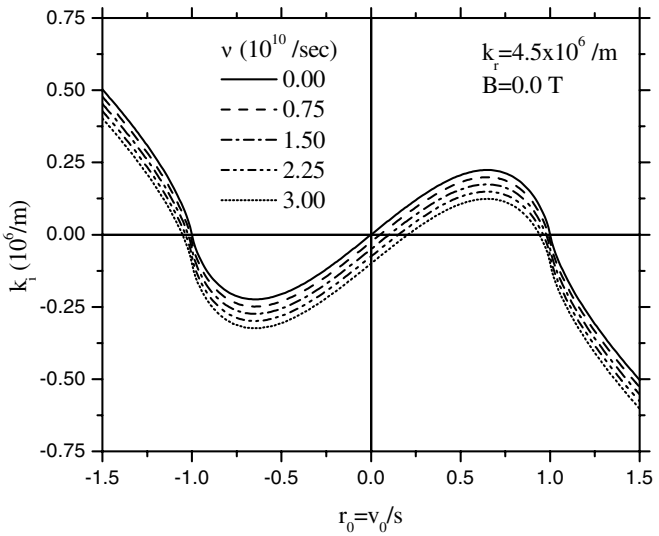

Figure 2. Plasma-wave increment k_i as a function of the Mach number $r_0 = V_0/s$, in the absence of a magnetic field. We use $L = 2\ \mu$m and $s = 1.5 \times 10^5$ m s^{-1} throughout. The other parameters used are shown in the figure. The steady flow is unstable when $0 < r_0 < 1$ and $r_0 < -1$.

correspond, respectively, to ν (in units of 10^{10} s^{-1}) equal to 0.00, 0.75, 1.50, 2.25, and 3.00. These values correspond to the parameters $L = 2\,\mu$m and $s = 1.5\times10^5$ m s^{-1} used throughout. The value of k_r is kept fixed ($k_r = 4.5 \times 10^6$ m^{-1}) for all cases considered. We recall that the steady flow is said to be unstable if $k_i > 0$ (or, in other words, if the plasma wave grows) and stable if $k_i < 0$. By this token, we note that for $r_0 > 0$, the steady flow is unstable if $0 < r_0 < 1$ and stable if $r_0 > 1$. For $r_0 < 0$ (or, in other words, if the boundary conditions at the source and drain are interchanged), the flow is unstable if $r_0 < -1$ and stable if $r_0 > -1$. Interestingly, the same conclusions were drawn in the absence of any external friction [4]. This then leads us to infer that the presence of an external friction decreases the wave increment but does not alter its characteristics. Moreover, such a decrement is seen to enhance with increasing friction. It is also important to note that the net effect of the external friction is to add a $-\nu/2$ term to the wave increment, just as was noted in reference [4].

Figure 3 depicts the wave increment as a function of the Mach number r_0 for different intensities of the magnetic field, B, keeping k_ν fixed such that $\nu = 1.5 \times 10^{10}$ s^{-1}. There are several noteworthy points. First, the shift of the wave increment is much larger in the presence of an applied magnetic field than in its absence, which has been estimated by a term $-\nu/2$ (see above). Second, all curves show different crossing points in the vicinity of $r_0 = \pm1$, unlike in the zero-ν case, where all curves are seen to pass through one and the same point at $r_0 = 0$ and $r_0 = \pm1$ (see, for example, the solid curve in figure 3). Third, it is clearly seen that the wave increment grows with increasing magnetic field in both regions ($r_0 < -1$ and $0 < r_0 < 1$) of instability. This implies that the role of an applied magnetic field is *additive* contrary to the zero-field case where the ν-induced instability is known to be *subtractive* with increasing ν.

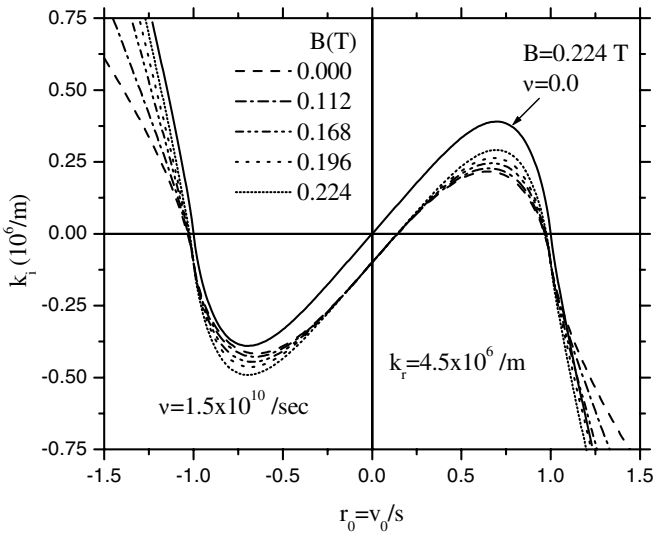

Figure 3. Plasma-wave increment k_i as a function of the Mach number r_0. The collisional frequency ν is fixed ($\nu = 1.5 \times 10^{10}$ s^{-1}) and the magnetic field (B) is varied. The solid curve refers to the reference curve with $\nu = 0.0$ and $B = 0.224$ T. Here k_r is kept fixed at $k_r = 4.5 \times 10^6$ m^{-1} for all the cases considered. Evidently, the role of the magnetic field is *additive*.

Figure 4 presents the absolute variation of the wave increment $|k_i|$ as a function of the magnetic field B. We investigate practically the more interesting region (with respect to r_0) [4] in both the zero-ν and nonzero-ν cases. The middle curve that represents the $\nu = 0$ case is seen to lie at the absolute average of the nonzero-ν curves. It is not surprising that the

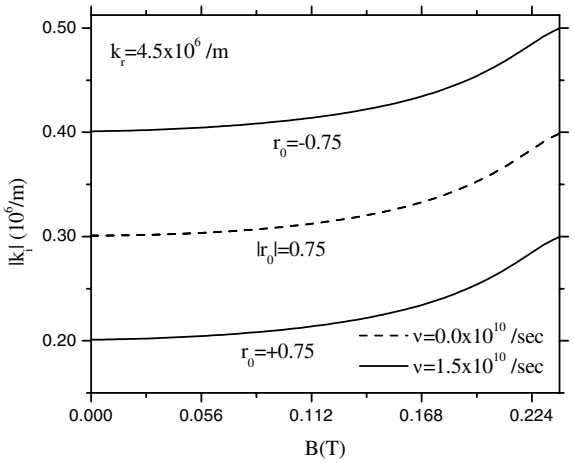

Figure 4. Absolute plasma-wave increment $|k_i|$ as a function of magnetic field B. The middle curve for $\nu = 0$ is, in this sense, symmetrical with respect to r_0, and represents both the stable and unstable regions. The ν-induced asymmetry is explained by the lower and the upper curves for $\nu \neq 0$.

magnitude of the $r_0 < 0$ curve (i.e., in the stable region) in the nonzero-ν case is higher than its $r_0 > 0$ counterpart (in the unstable region). This is attributed to the ν-induced shift towards the $k_i < 0$ region in the third quadrant of figure 3, for example. Interestingly, the absolute magnitude of the variation in k_i is observed to increase, both in the stable and unstable regions, with increasing magnetic field.

Figure 5 illustrates the wave increment as a function of the Mach number r_0 for a given intensity of the magnetic field $B = 0.224$ T. There are various points worth mentioning. Only

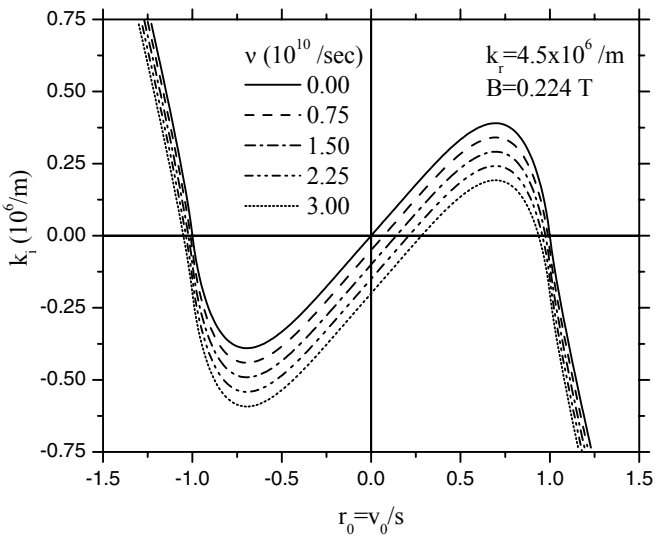

Figure 5. Plasma-wave increment k_i as a function of the Mach number r_0. The collisional frequency ν is varied while the magnetic field B is kept fixed. The parameters are as listed inside the figure.

the $\nu = 0$ curve is observed to pass exactly through the $r_0 = 0$ and $r_0 = \pm 1$ points; the rest of the curves follow their own trajectories. Just as in the zero-field case, the instability (stability) of the plasma wave decreases (increases) in magnitude with increasing ν. Mathematical complexity prevents us from estimating exactly the shift of the wave increment/decrement in the presence of an applied magnetic field. However, the illustrative examples reveal that this shift is larger in the presence of a magnetic field than in its absence.

Figure 6 shows the absolute variation of the wave decrement (increment) in the unstable (stable) regions as a function of collision frequency ν. Our numerical results, subject to the approximation imposed in equation (22), reveal that the said variation is almost linear. This figure simply encapsulates the conclusions drawn from figure 5.

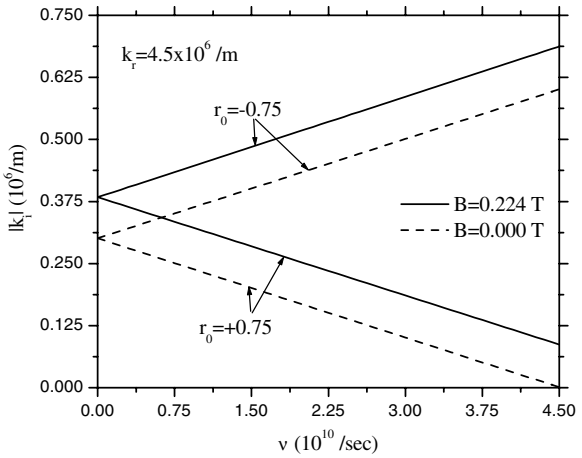

Figure 6. Absolute plasma-wave increment $|k_i|$ as function of the collisional frequency ν. The ν-induced asymmetry is evident throughout, except at $\nu = 0$, where the respective curves become degenerate. The parameters used are as listed in the figure.

Finally, figure 7 illustrates a three-dimensional plot of the wave increment $2k_iL$ as a function of the magnetic field k_cL and the Mach number r_0. This figure reveals a clear-cut evolution of the wave increment as both the magnetic field and the Mach number are varied simultaneously. The values of k_r and ν are kept fixed as $k_r = 4.5 \times 10^6$ m^{-1} and $\nu = 1.5 \times 10^{10}$ s^{-1} throughout. It is worth specifying that k_cL, r_0, and $2k_iL$ represent, respectively, the x-, y-, and z-axes of the 3D figure. A guide to how to view the figure is as follows. Looking at the y–z plane, for example, one is furnished with an extended view of what one sees in figure 3. Similarly, looking at the x–z plane one sees curves reminiscent of the collection of numerous such curves seen in figure 4. The surface plot in figure 7 is also seen to maintain its characteristic features, notable at $r_0 = 0$ and in the vicinity of $r_0 = \pm 1$, where the wave increment is, respectively, nonzero and zero for any value of the magnetic field.

4. Discussion

We have studied the wave increment in a 2D electron plasma realizable in a short FET channel, owing to the wave's reflection from the device boundaries, in the presence of an external friction and/or of a *weak* magnetic field. We have demonstrated that while the role of the external friction is *subtractive*, the magnetic field plays an *additive* role. This means that, for a given magnitude of the external friction, we expect the magnetic field to not only compensate

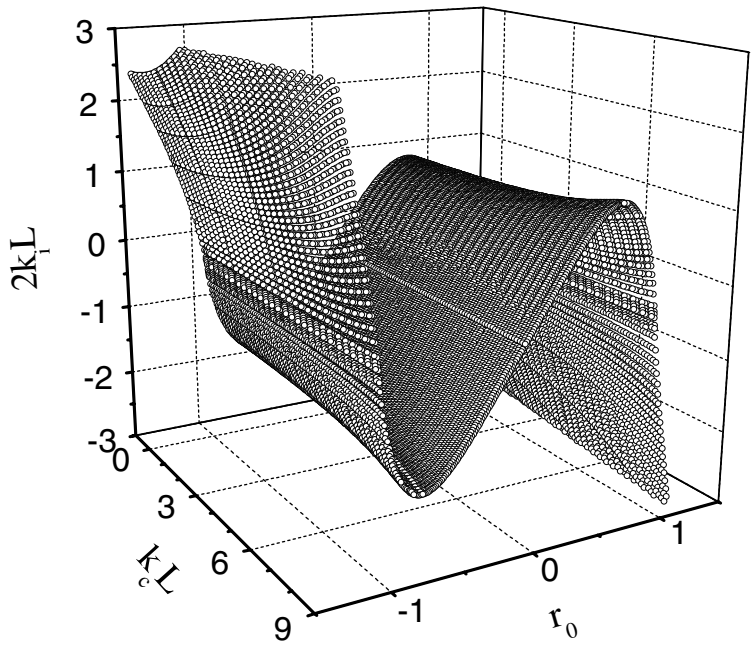

Figure 7. A three-dimensional plot of the dimensionless plasma-wave increment $2k_i L$ as a function of the dimensionless magnetic field $k_c L$ and the Mach number r_0. Here k_r is kept fixed at $k_r = 4.5 \times 10^6$ m^{-1} and ν at $\nu = 1.5 \times 10^{10}$ s^{-1}. This figure maintains, in a broad sense, all the behavioural characteristics of figures 3 and 4.

the resulting decrement in the wave growth but also to overcome it. What one would do then is adjust the intensity of the magnetic field in order to bring about the desired effect. In spite of such favourable conditions, there is one more mechanism that opposes it. This is the internal friction brought about by the viscous force due to the electron–electron scattering in the 2D plasma. The viscosity μ is known [4] to cause an additional damping with the decrement of the order of μq^2, where $q \equiv k_r$. Hence the viscosity is especially effective in damping higher-order modes.

We believe that an exact theoretical treatment of the external and internal frictions will probably give a better insight into the problem. In addition, since the 2D electron fluid is describable by equations analogous to those for shallow water waves, various hydrodynamic phenomena, such as wave and soliton propagation, the choking effect, and hydraulic jumps, should take place.

Finally, a few words are in order on some closely associated but unresolved aspects of the problem, which are still to be addressed in order for a successful observation of this instability mechanism to occur. The appropriateness of the asymmetric boundary conditions, the coupling between the electromagnetic radiation and the plasma waves, and the size effects due to the transverse dimension need to be better understood.

Acknowledgments

This work was supported by the NSERC grant No OGP0121756. The work of MSK was also supported by CONACyT Grant No 28110-E.

References

[1] Shur M S and Eastman L F 1979 *IEEE Trans. Electron. Devices* **26** 1677
[2] Heiblum M, Nathan M I, Thomas D C and Knoedler C M 1985 *Phys. Rev. Lett.* **55** 2200
[3] Chao P C, Shur M, Tiberio R C, Duh K H G, Smith P M, Ballingall J M, Ho P and Jabra A A 1989 *IEEE Trans. Electron. Devices* **36** 461
[4] Dyakonov M and Shur M 1993 *Phys. Rev. Lett.* **71** 2465
[5] Dyakonov M I and Shur M S 1995 *Phys. Rev.* B **51** 14 341
[6] Brodkey R S 1967 *The Phenomena of Fluid Motion* (Reading, MA: Addison-Wesley)
[7] Gelmont B 1995 *Proc. Int. Semiconductor Device Research Symp. (Engineering Academic Outreach, University of Virginia, Charlottesville, VA, 1995)* vol 2, p 559
[8] Streeter V L and Wylie E B 1985 *Fluid Mechanics* (New York: McGraw Hill)
[9] Dmitriev A P, Furman A S and Kachorovskii V Yu 1996 *Phys. Rev.* B **54** 14 020
[10] Dmitriev A P, Furman A S, Kachorovskii V Yu, Samsonidze G G and Samsonidze Ge G 1997 *Phys. Rev.* B **55** 10 319
[11] Shur M S and Lü J Q 2000 *IEEE Trans. Electron. Devices* **48** 750